Molecular Therapy
Methods & Clinical Development
Original Article

Optimization of AAV6 transduction enhances site-specific genome editing of primary human lymphocytes

Geoffrey L. Rogers,[1] Chun Huang,[1] Robert D.E. Clark,[1] Eduardo Seclén,[1] Hsu-Yu Chen,[1] and Paula M. Cannon[1]

[1]Department of Molecular Microbiology and Immunology, Keck School of Medicine, University of Southern California, Los Angeles, CA, USA

Adeno-associated virus serotype 6 (AAV6) is a valuable reagent for genome editing of hematopoietic cells due to its ability to serve as a homology donor template. However, a comprehensive study of AAV6 transduction of hematopoietic cells in culture, with the goal of maximizing *ex vivo* genome editing, has not been reported. Here, we evaluated how the presence of serum, culture volume, transduction time, and electroporation parameters could influence AAV6 transduction. Based on these results, we identified an optimized protocol for genome editing of human lymphocytes based on a short, highly concentrated AAV6 transduction in the absence of serum, followed by electroporation with a targeted nuclease. In human CD4$^+$ T cells and B cells, this protocol improved editing rates up to 7-fold and 21-fold, respectively, when compared to standard AAV6 transduction protocols described in the literature. As a result, editing frequencies could be maintained using 50- to 100-fold less AAV6, which also reduced cellular toxicity. Our results highlight the important contribution of cell culture conditions for *ex vivo* genome editing with AAV6 vectors and provide a blueprint for improving AAV6-mediated homology-directed editing of human T and B cells.

INTRODUCTION

Ex vivo genome editing of hematopoietic cells has now advanced to the clinic as a treatment for several human genetic and infectious diseases.[1] The target cells include hematopoietic stem and progenitor cells (HSPCs), capable of reconstituting an entire immune system, as well as more differentiated subsets such as T cells and B cells. One of the most well-studied methods for editing hematopoietic cells combines the transient delivery of a targeted nuclease with transduction of a homology donor DNA template packaged in an adeno-associated virus (AAV) vector.[2–4] The targeted nuclease is designed for only transient expression, delivered for example by electroporation of zinc-finger nuclease (ZFN) mRNA or Cas9 ribonucleoprotein complexes (RNP). Following introduction of a site-specific break in the targeted chromosomal site, the cellular homology-directed repair (HDR) pathway uses the supplied AAV genome to permanently incorporate modified DNA at that site.[5–7] These procedures can result in high-frequency modification of hematopoietic cells, with editing efficiencies ranging from 20% to 80% across cell types and genomic loci.[2,8–20]

In developing protocols for genome editing of hematopoietic cells, significant effort has been expended on the targeted nuclease: developing platforms for efficient transient delivery,[2,4,21,22] optimizing protein sequences,[23] and chemically modifying RNA components[24] to maximize on-target nuclease activity while minimizing potentially deleterious off-target DNA break formation. Additional improvements in HSPC genome editing have focused on identifying culture conditions that facilitate HDR through the manipulation of the cell cycle or DNA repair pathways,[21,25,26] as well as to retain optimal stemness and proliferative potential after engraftment.[8,11,12,21,27] In contrast, less attention has been paid to conditions that could affect the delivery of the homology donor DNA using AAV vectors.

The efficacy and safety of AAV for gene delivery is well-studied. The parental virus is a small, nonpathogenic parvovirus, encapsidating a single-stranded DNA genome of about 4.7 kb.[28] For recombinant vectors, all viral DNA sequences are removed other than the inverted terminal repeats (ITRs) necessary for genome packaging into the capsid. AAV vectors have been used extensively in both preclinical and clinical studies, and two products for the treatment of monogenetic disorders are currently approved by the US Food and Drug Administration (FDA).[29,30] AAV is particularly versatile as a gene therapy vector due to its relatively low immunogenicity, the variety of serotypes available with tropism for different tissues, and the ability to persist as episomal, nonintegrated DNA for upward of a decade.[31] As such, most work using AAV has focused on *in vivo* gene delivery, with *ex vivo* applications for AAV, including as a template for HDR genome editing, comparatively less established.

Screening in human HSPCs,[2,32,33] T cells,[3,13] and B cells[16] identified AAV6 as an effective serotype for transduction *ex vivo* in all three hematopoietic cell lineages. Some recent studies have also reported reagents that may enhance uptake of AAVs, including AAV6, in

Received 19 April 2021; accepted 3 September 2021;
https://doi.org/10.1016/j.omtm.2021.09.003.

Correspondence: Paula M. Cannon, PhD, Department of Molecular Microbiology and Immunology, Keck School of Medicine, University of Southern California, 2011 Zonal Ave, HMR 413A, Los Angeles, CA 90033, USA.
E-mail: pcannon@usc.edu

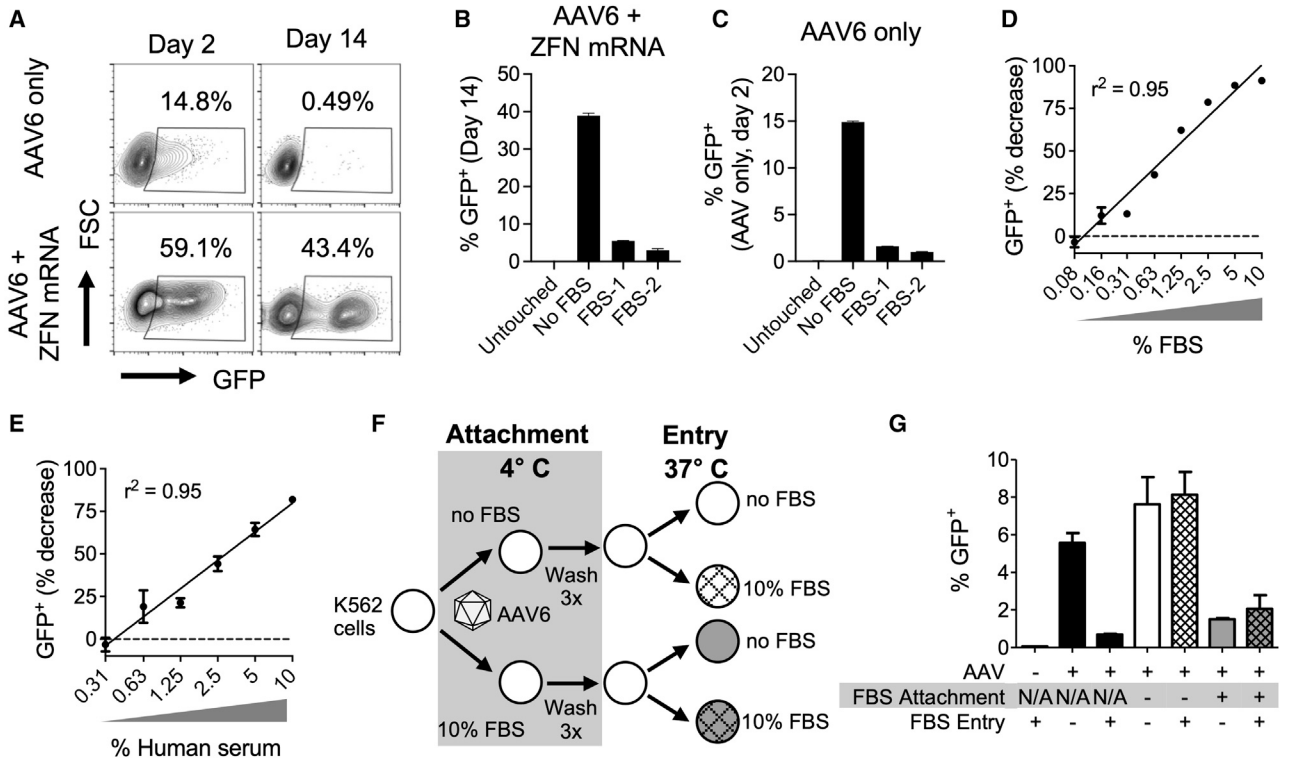

Figure 1. Cell culture serum inhibits AAV transduction

(A–C) K562 cells were nucleofected or not with *CCR5* ZFN mRNA and then transduced with MOI = 10^4 AAV6-CCR5-GFP vectors. Cells were transduced at 10^6 cells/mL with or without 2 different batches of 10% FBS for 2 h before 10% FBS is restored for further culture. (A) Representative plots of GFP expression after 2 and 14 days by flow cytometry. (B) Quantification of GFP expression in cells treated with ZFN mRNA and AAV6 vectors after 14 days. (C) Quantification of GFP expression in cells treated with AAV6 vectors alone after 2 days. Data for (B) and (C) are mean ± SEM for n = 2 technical replicates. (D and E) Inhibition of AAV6 transduction as for (A) by MOI = 10^4 of K562 cells was calculated over a range of serum concentrations for FBS-3 (D) or human AB serum (E), and a semi-logarithmic regression line was calculated. Data are mean ± SEM for n = 3 technical replicates. (F and G) A viral attachment assay was performed for MOI = 10^4 AAV6-CCR5-GFP vectors on K562 cells, as diagramed (F), and GFP expression was measured after 2 days by flow cytometry (G). Bar colors correspond to treatments, and black bars are control samples transduced at 37°C without prior attachment. Data are mean ± SEM for n = 3 technical replicates.

hepatocytes or human HSPCs.[34,35] However, comprehensive work has not been published to optimize the factors that could affect AAV transduction of hematopoietic cells *ex vivo* and thereby influence genome editing outcomes. Here, we report an improved protocol for AAV6 delivery as part of nuclease-mediated genome editing, resulting in improved editing efficiencies in T cells and B cells, while also reducing cellular toxicity.

RESULTS

Fetal bovine serum inhibits genome editing with AAV6 donors

To potentially improve the delivery of homology donor templates based on AAV6 vectors, we first assessed the impact of fetal bovine serum (FBS) concentration in cell culture conditions. Wang et al.[13] previously reported that transduction of primary human $CD3^+$ T cells with AAV6 in FBS-free conditions improved site-specific genome editing when using multiplicities of infection (MOIs) of 10^4–3×10^5 compared to transduction in media supplemented with 10% FBS. To further test this, we performed genome editing in K562 cells in the presence or absence of 2 different lots of FBS, using *CCR5* gene editing reagents that are well-validated by our group. They comprise AAV6 homology donor vectors containing a GFP expression cassette (AAV6-CCR5-GFP) and matched *CCR5*-specific ZFN mRNAs, which result in site-specific insertion of the GFP expression cassette at *CCR5*.[2,36] In the absence of FBS, the combination of AAV6 donors and ZFN mRNAs resulted in stable GFP expression at day 14 in about 40% of cells, whereas cells that received AAV6 only were <1% GFP^+ (Figure 1A). This high level of stable GFP expression in cells that received both AAV6 and ZFN mRNA is indicative of site-specific genome editing, as we have previously characterized.[2,36] In contrast, when ZFN-treated cells were transduced with AAV6 in the presence of FBS, editing rates at day 14 were reduced by approximately 90% for both FBS batches (Figure 1B). In cells transduced with AAV6 but not electroporated with ZFN mRNA, where GFP expression resulted from vector transduction alone, the patten of expression at day 2 mirrored that for the genome editing conditions, suggesting that the reduced rates of editing we observed in the presence of FBS were a consequence of impaired AAV6 transduction (Figure 1C).

Cell culture with serum inhibits AAV6 transduction by reducing vector attachment

To further investigate the impact of FBS on AAV6 transduction, we next transduced a variety of suspension and adherent cell lines with AAV6 vectors containing the same GFP expression cassette (AAV6-CCR5-GFP)[2] at MOIs of 10^3–10^6 and quantified any inhibition by 10% FBS (Figure S1). We observed 78%–98% inhibition at the lowest MOIs tested, whereas inhibition was only 0%–36% at the highest MOIs. This suggests that the inhibitory factor in FBS is dose-limiting and can be out-competed by excess AAV6. Heat inactivation of FBS had no effect on inhibition of AAV6 transduction, suggesting that complement is not involved in this process (Figure S2).

A titration of FBS concentration during AAV6 transduction of K562 cells at the susceptible MOI of 10^4 revealed that the inhibitory effect was both potent and dose-dependent (Figure 1C). Near-complete inhibition was observed at the standard culture concentration of 10% FBS, and some inhibition persisted until FBS was diluted to less than 0.1% of the culture media present during transduction.

Since clinical protocols generally eschew FBS to avoid potential contamination with animal proteins, we also measured the anti-AAV6 activity of a single batch of human AB serum. The human serum exhibited a similar dose-response curve against AAV6 as was observed with the batch of FBS tested (Figure 1D), suggesting that this effect is likely not restricted to fetal bovine sources of serum.

Next, we investigated the generalizability of this finding across different AAV serotypes. We used 293T cells, which are permissive for AAV1, AAV2, and AAV6 at an MOI of 10^4. AAV6 transduction was inhibited by 4 different batches of 10% FBS, with decreases in GFP expression ranging from 25%–52% (Figure S3A). In contrast, significantly more variability was observed with serotypes AAV1 and AAV2, where batch FBS-4 was >75% inhibitory, but FBS-5 and -6 produced minimal inhibition (Figures S3B and S3C). The single batch of human AB serum was more strongly inhibitory against all 3 AAV serotypes tested than any of the batches of FBS (Figure S3), suggesting that replacing the serum source could not ablate serum-mediated inhibition of AAV transduction. Overall, these results suggest that inhibition of AAV transduction by FBS and human serum is observed across several AAV serotypes and is not a specific phenomenon of AAV6 vectors.

Finally, to investigate the mechanism of AAV6 inhibition by FBS, we performed a viral attachment assay. Here, K562 cells are incubated with AAV6 at 4°C to allow viral attachment but not entry, followed by thorough washing and then additional incubation at 37°C to permit uptake of any attached viral particles (Figure 1E).[37] As previously observed, AAV6 transduction in control samples maintained throughout at 37°C was inhibited by FBS, and this was also observed when FBS was present during the 4°C attachment step (Figure 1F). In contrast, allowing AAV6 to first attach to cells at 4°C in the absence of FBS resulted in transduction, regardless of whether FBS was present during the subsequent 37°C incubation. Together, these results suggest that FBS inhibits AAV6 transduction by preventing attachment of the vector to cells rather than acting to prevent viral uptake, or through any changes in cell permissivity at post-entry stages of transduction.

Impact of culture volume and time on AAV6 transduction

In AAV transduction protocols, MOI is frequently the only characteristic that is reported. However, there are a number of other variables that could impact transduction with the same ratio of cells and AAV vector genomes. For instance, Ling et al.[38] previously reported that increasing cell density during AAV6 exposure improved transduction in both K562 cells and human $CD34^+$ HSPCs. To further test this, we transduced equal numbers of K562 cells with AAV6 MOIs ranging from 10^3 to 10^6 and using a range of different culture volumes (Figure 2A). While MOI was clearly an important driver of transduction rates, at each MOI greater than 10^3, reducing the culture volume also significantly enhanced transduction. These enhancements were sufficient to achieve comparable or superior AAV6 transduction with 10-fold lower MOIs for several comparison points. For example, an MOI of 10^4 in 5 μL produced 26.6% GFP^+ cells, but using 500 μL of culture required an MOI of 10^5 to produce only 20.9% GFP^+ cells. Interestingly, this impact of culture volume on AAV6 transduction rates was more dramatic at higher MOIs (Table S1), which likely reflects the rules of Brownian motion that govern interactions between viruses and cells in solution.[39]

As a consideration for AAV6 transduction in the absence of FBS, we were also interested to identify culture times that could optimize transduction while minimizing the deleterious effects of serum starvation on cell viability. Transducing K562 cells at a standard MOI of 10^4, and in a cell concentration of 10^6 cells/mL, revealed a biphasic pattern of AAV transduction over time. Specifically, the frequency of GFP^+ cells increased logarithmically in the first hour or so (Figure 2B), whereas a linear rate of transduction was observed thereafter up to 24 h of exposure (Figure 2C). As anticipated, increasing the cell concentration 10-fold to 10^7 cells/mL while maintaining the MOI of 10^4 enhanced transduction at all time points tested (compare Figure 2C and Figure 2D). Interestingly, regression analysis suggested that the linear rate of transduction was unaltered by the reduced volume, as the slope of the linear regression was not significantly different between the two datasets (Table S2). A lower MOI of 10^3 significantly altered the slope of the linear regression but still appeared to display the biphasic rate of transduction (Figure 2D; Table S2).

Finally, to investigate the physical entry of AAV6 vectors into cells over time, we performed a vector copy number (VCN) analysis on transduced cells. The number of cell-associated AAV genomes showed a strong linear correlation with the percentage of GFP^+ cells across the different transduction conditions (Figure 2E), suggesting that the rate of AAV6 transduction over time is regulated by cellular entry of viral particles. Together, these results suggest that the benefits of AAV6 transduction in a low volume of media are realized in the first 1–2 h of exposure, during the logarithmic stage of the biphasic transduction observed.

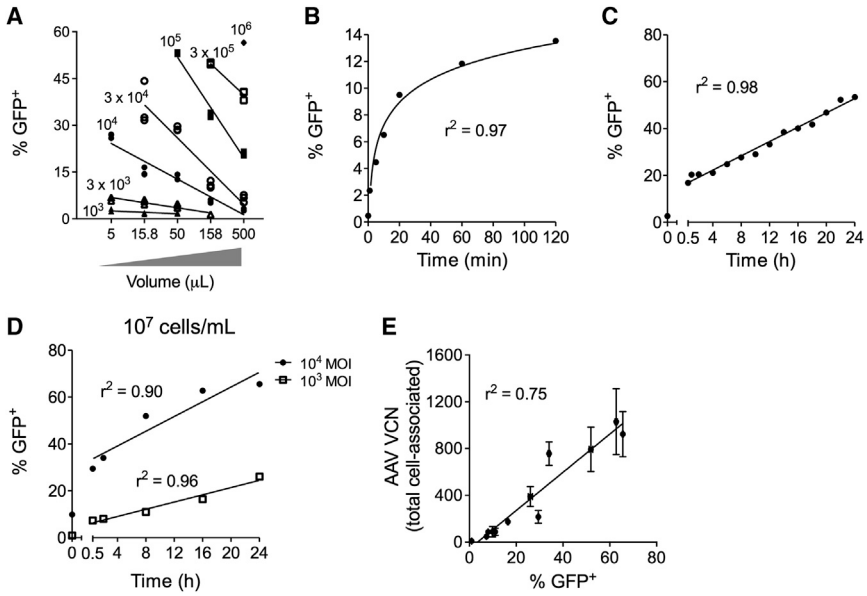

Figure 2. Effects of culture volume and time on AAV6 transduction

(A) The combined influences of AAV MOI and cell culture volume on AAV6 transduction of K562 cells were evaluated. 5 × 10^4 K562 cells were transduced with AAV6-CCR5-GFP at MOIs of 10^3–10^6 in the indicated volumes for 2 h prior to addition of 10% FBS, and GFP expression was measured after 2 days by flow cytometry. Graph shows each individual replicate for n = 3. MOIs are as indicated on the graph: 10^3 = closed triangle, 3 × 10^3 = open triangle, 10^4 = closed circle, 3 × 10^4 = open circle, 10^5 = closed square, 3 × 10^5 = open square, 10^6 = closed diamond. See also Table S1 for regression characteristics. (B and C) K562 cells were transduced with AAV6 at 10^6 cells/mL and an MOI of 10^4 for the indicated times. Transduction was halted by 10% FBS, and GFP expression was measured after 2 days. (B) shows that transduction over the first 2 h fits a semi-logarithmic regression, while (C) illustrates an initial jump in transduction followed by increases that fit a linear regression starting 0.5 h after transduction. (D) Transduction of K562 cells over time with AAV6 at a higher concentration of 10^7 cells/mL and MOIs of 10^4 or 10^3 was performed as before. See also Table S2 for regression characteristics. (E) Cell-associated AAV vector copy numbers (VCNs) were measured for cells in (D) by ddPCR, and a linear regression was used to measure correlation between GFP expression and VCN. Data in (B)–(E) are shown as mean ± SEM for n = 3 technical replicates.

Electroporation enhances AAV6 transduction

Electroporation to introduce a targeted nuclease is an additional step in *ex vivo* genome editing protocols that is not performed during AAV transductions. A previous study by Charlesworth et al.[21] suggested that recently electroporated cells are more permissive to AAV6 transduction due to a general enhancement of cellular endocytosis. In agreement, we found that electroporation of K562 cells prior to addition of AAV6 enhanced transduction; however, this was still strongly inhibited by 10% FBS (Figure 3A). Moreover, this effect was also observed when cells were transduced with AAV6 prior to electroporation (Figure 3B). FBS was again partially inhibitory, although electroporation rescued transduction to levels comparable to cells transduced without electroporation or FBS. Washing cells to remove AAV6 prior to electroporation did not affect the electroporation enhancement of transduction, suggesting that the AAV6 particles already attached to cells are more efficiently able to transduce cells after electroporation, rather than direct membrane permeation by free AAV. Last, we confirmed that electroporation prior to AAV6 exposure was also able to enhance transduction in primary human $CD4^+$ T cells and $CD34^+$ HSPCs (Figures 3C and 3D). Together these results suggest that electroporation enhances AAV transduction of both cell lines and primary human cells, likely through an enhancement of viral uptake, regardless of the sequence of events.

An optimized AAV6 transduction protocol for nuclease-mediated genome editing

Having identified several parameters that impact AAV6 transduction, we next explored whether optimization of these variables could improve site-specific genome editing by AAV6 homology donors. We aimed to take advantage of the positive effects we had observed of performing AAV6 transduction in small volumes of media, and the ability of electroporation to enhance AAV6 entry regardless of the relative timing of AAV6 incubation or electroporation.

Guided by our prior observations, we designed an optimized protocol for genome editing whereby K562 cells were thoroughly washed to remove FBS from culture media, transduced in serum-free media at high concentration of cells (10^7/mL) using an AAV6-CCR5-GFP MOI of 10^4 for 1 h, and then electroporated with *CCR5*-specific ZFN mRNA and immediately resuspended in media containing 10% FBS (Figure 4A; Table 1). A 1 h transduction was chosen to capture the initial exponential phase of AAV transduction while minimizing the deleterious impacts of serum starvation and high-density culture. We contrasted this with a more standard genome editing protocol that involved first electroporating the ZFN mRNA, followed by transduction of cells at a concentration of 10^6/mL and using an AAV6 MOI of 10^4 for 2 h in FBS-free media, before the addition of 10% FBS. We observed that the optimized protocol edited 51.1% of cells compared to 39.6% with the original protocol, even though the same amounts of cells, AAV6 vectors, and ZFN mRNA were used in each case (Figure 4B).

We also assessed the impact of the FBS-free transduction period on genome editing rates by transducing the K562 cells for either 1 or 24 h prior to electroporation with ZFN mRNA and varying the cell concentration. Improvements were observed for the 24 h transduction period at MOIs of both 10^4 and 10^3, which could also be achieved by increasing the cell concentration to 5 × 10^7 cells/mL at the lower

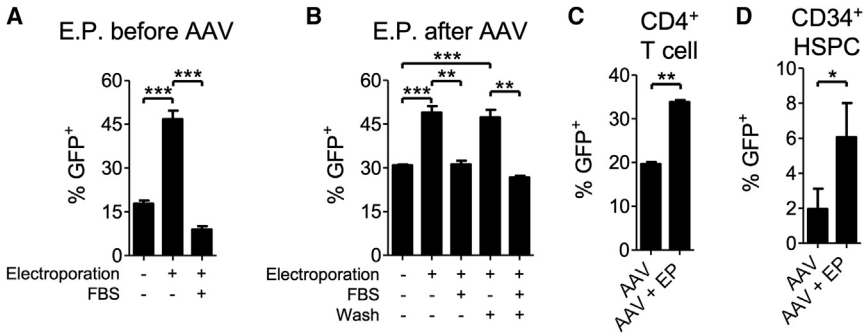

Figure 3. Electroporation enhances transduction by attached AAV6 particles

(A and B) K562 cells were transduced with AAV6-CCR5-GFP vectors at 10^6 cells/mL and an MOI of 10^4, and GFP expression was measured after 2 days by flow cytometry for n = 3 technical replicates. Electroporation was performed either before (A) or after (B) AAV6 transduction. Washing was performed with PBS after transduction as indicated, and for cells not transduced in the presence of FBS, media was supplemented with 10% FBS after 2 h or after electroporation. (C) $CD4^+$ T cells from n = 2 human donors were transduced with AAV6-CCR5-GFP at an MOI of 10^4 with or without prior electroporation, and GFP expression was measured after 2 days by flow cytometry. (D) HSPCs from n = 3 donors were transduced with AAV6-CCR5-GFP at an MOI of 3×10^3 with or without prior electroporation, and GFP expression was measured after 1 day by flow cytometry. Data are shown as mean ± SEM. *p < 0.05; **p < 0.01; ***p < 0.001.

MOI with only 1 h incubation (Figure 4B). However, we consider that a 1 h transduction is likely to be the best choice for primary cells, since this will minimize the duration of serum starvation.

Improved genome editing in primary human $CD4^+$ T cells

We next evaluated genome editing in primary human $CD4^+$ T cells, comparing a protocol based on previously published procedures[13,14] with our optimized protocol using concentrated AAV6 transduction in FBS-free media for 1 h prior to electroporation (Figure 4A; Table 1). With both protocols, stable GFP expression indicative of site-specific genome editing was observed only in cells that received both ZFN mRNA and AAV6 (Figures 5A, S4A, and S4B). However, the optimized protocol yielded 2.2- to 6.7-fold higher editing levels across a range of MOIs (Figure 5B). Significantly, the 33.3% average rate of editing achieved using the optimized protocol at the lowest MOI was greater than the 29.9% editing rate achieved with the previously published protocol at the highest MOI used (Figure 5B), despite our protocol using 50-fold less AAV6. Moreover, no differences were observed in the insertion or deletion (indel) frequencies in cells electroporated with ZFN mRNA alone, suggesting that the optimized protocol did not impact electroporation efficiency or nuclease activity (Figure 5C).

Interestingly, the higher levels of genome editing obtained with the optimized versus original protocols could not be predicted simply by comparing the rates of AAV6 transduction in the absence of a targeted nuclease. Indeed, despite achieving higher editing levels at day 10, AAV6 transduction was significantly lower at day 2 using the optimized protocol when compared to the original protocol at the highest MOI for each. This potentially reflects differences in AAV6 MOI (original = 5×10^4, optimized = 10^4) and transduction time (original = overnight, optimized = 1 h) between the two methods (Figure 5D). In addition, at the day 2 time point, we did not observe enhanced proliferation in cells transduced with the optimized protocol that could have resulted in more rapid dilution of the episomal AAV6 genome (Figure S5). Interestingly, the transduction rates of about 5%–10% (Figure 5D) when using the optimized protocol were also significantly lower than the final genome editing rates achieved of about 40%–60% (Figure 5B). This discrepancy may reflect differences in the sensitivity of the readouts, since the intensity of GFP expression from edited cells is significantly higher than in cells transduced with AAV6 alone (Figures 5A and S4A), as noted in a previous report that higher GFP expression rates could be used to enrich for gene-edited cells following editing with AAV6 homology donors.[4] In this way, it is likely that GFP reporters may not accurately capture weak or transient episomal expression after transduction by AAV vectors[40] and suggests that AAV transduction rates measured by GFP reporters may not be an absolute measure of the genome editing potential of a cell.

As an alternative explanation, improved cell viability was observed 1 day after electroporation in cells edited with the optimized protocol, although no significant difference in $CD4^+$ T cell numbers was observed at this time point (Figures 5E, 5F, S6A, and S6B; Table S3). It is possible that improved cell health allows higher rates of genome editing, since the DNA repair pathways necessary for HDR are only active during the G2/S phases of the cell cycle.[25,41]

Finally, we observed a cap on genome editing rates with increasing AAV6 MOIs using the optimized protocol. A 9-fold increase in the AAV6 MOI (from 10^4 to 9×10^4) with the optimized protocol was unable to further increase genome editing rates (Figure 5G). To achieve this MOI, cells were transduced in undiluted AAV6 vector, which resulted in a decrease in viability from 81% to 73% (not shown) and so may be inappropriate for routine use. These data suggest that an effective maximum rate had been reached based on additional restrictions on genome editing efficiency.

Improved genome editing in primary human B cells

We next evaluated whether the optimized AAV6 transduction protocol could improve genome editing rates in primary human B cells, which we have previously found to require AAV6 MOIs of 10^6 and above for efficient site-specific gene insertion with an original protocol adapted from methods in T lymphocytes[13,14] (Figure 4A; Table 1). Similar to the $CD4^+$ T cells, we found that genome editing in primary B cells required ZFN mRNA (Figures 6A, S4C, and S4D) and was greatly enhanced by the optimized protocol, up to 21.1-fold at equal

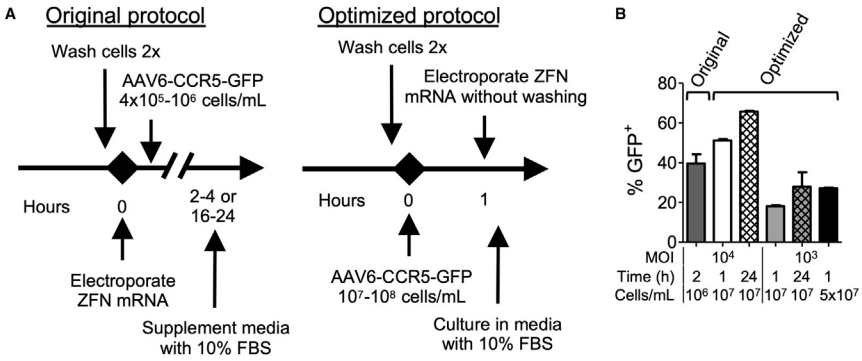

Figure 4. An optimized AAV6 transduction protocol enhances genome editing in K562 cells

(A) Diagram of the original and optimized protocols. In the original protocol, cells are electroporated first, then transduced with AAV6-CCR5-GFP using standard cell culture concentrations prior to addition of FBS. In the optimized protocol, cells are transduced with AAV6-CCR5-GFP at high cell concentrations prior to electroporation, then cultured under standard conditions with FBS supplementation. See Table 1 and supplemental methods for additional details of each protocol in specific cell types. (B) K562 cells were genome edited using the original protocol (far left bar) involving AAV6-CCR5-GFP transduction for 2 h after electroporation of ZFN mRNA, or the optimized protocol with varying parameters of MOI, time, and cell concentration as indicated below. Data are shown as mean ± SEM for n = 2 technical replicates.

MOIs (Figure 6B). Although the overall maximum rates of editing achieved were the same for both protocols, equal frequencies of GFP^+ edited cells were achieved using 10-fold less AAV6 in the optimized protocol, and with only a slight, non-statistically significant reduction observed with 100-fold less AAV6 (Figure 6B). In contrast to $CD4^+$ T cells, transduction of B cells in the absence of a targeted nuclease was slightly improved by the optimized protocol, although this was not statistically significant (Figure 6C). Last, as before, a significant survival advantage was observed with the optimized protocol in terms of B cell viability, as well as the total number of cells remaining 1 day after electroporation (Figures 6D, 6E, S6C, and S6D; Table S3). Therefore, the optimized protocol allowed for major reductions in the amount of AAV6 vectors required to achieve efficient rates of genome editing in human B cells, although additional barriers beyond AAV6 delivery still appear to limit the maximum genome editing rates that can be achieved in this cell population.

Genome editing in $CD34^+$ HSPCs is unaffected by the optimized AAV6 transduction protocol

Finally, we investigated whether the optimized protocol for AAV6 transduction could also improve editing in $CD34^+$ HSPCs using our previously reported method combining AAV6 transduction with electroporation of ZFN mRNAs (Figure 4A; Table 1).[2] Bulk $CD34^+$ HSPCs containing a mixture of stem and progenitor cells have historically required lower AAV6 MOIs for efficient genome editing than human lymphocytes.[2,13] Interestingly, although editing again required ZFN mRNA (Figures 7A, S4E, and S4F), no differences in editing rates were observed between the two transduction protocols across a range of MOIs (Figure 7B). Transduction rates in the absence of a targeted nuclease, measured at day 1, were also similar between the 2 protocols (Figure 7C). There was a slight but significant advantage in cellular viability with the optimized protocol, but no difference in cell numbers was noted by 1 day after electroporation (Figures 7D, 7E, S6E, and S6F; Table S3). The overall low viability of HSPCs at this time point (~30%–40%) was mainly a characteristic of the fetal liver-derived cell population, as untreated cells were only around 55% viable at day 1, and the further loss of cell viability appeared to be related mainly to mRNA electroporation rather than a specific consequence of editing (Figure S7). In all samples, viability recovered to expected levels after prolonged culture (not shown). Thus, despite its impact in primary human lymphocytes, the optimized AAV6 transduction protocol did not appreciably enhance genome editing in $CD34^+$ HSPCs.

DISCUSSION

AAV vectors are invaluable reagents for site-specific genome editing of human hematopoietic cells, with AAV6 serotypes in particular being widely used to deliver homology donors to HSPCs,[2,4,11,12] T cells,[13–15] and B cells.[16,17,19] The *in vitro* tropism of AAV6 for human hematopoietic cells,[2,13,16] as well as its weak induction of innate immune pathways that could trigger harmful biological consequences in engineered cells,[42,43] may contribute to its success. In addition, the vector's ability to transduce both dividing and quiescent cells[44] may also be beneficial, particularly if the genome is used as a homology template only after second-strand synthesis as some have suggested,[7] though the G2/S phase restriction of cellular factors required for HDR[25] may limit the advantages conferred by this attribute.

Despite using similar protocols, we and others have observed relative inefficiencies in AAV6 transduction and genome editing for human lymphocytes compared to HSPCs. In this study we chose to focus on optimizing culture conditions for AAV6 transduction of suspension cells *ex vivo*, hypothesizing that achieving efficient delivery of the homology template may be (one of) the rate-limiting steps in these experiments.

Our initial experiments focused on the impact of serum on AAV transduction, based on reports that FBS could be inhibitory.[13] We observed dose-dependent inhibition of AAV6 transduction with both fetal bovine and human serum, which functioned by blocking AAV6 attachment to target cells. Inhibition by serum varied across different lots of FBS and AAV serotypes and was observed despite differing use of glycan receptors between the serotypes tested (AAV1: sialic acid; AAV2: heparan sulfate proteoglycan; AAV6: both).[28] This variance in neutralization across serum origins and lots, and AAV serotypes, is consistent with the presence of anti-AAV neutralizing antibodies (NABs). NABs to therapeutically

Table 1. AAV6 transduction parameters for original and optimized protocols in each cell type

Cell type	Transduction parameter	Original protocol	Optimized protocol
K562 cells	concentration (cells/mL)	10^6	$1–5 \times 10^7$
	time (h)	2	1 or 24
$CD4^+$ T cells	concentration (cells/mL)	10^6	10^8
	time (h)	16–24	1
B cells	concentration (cells/mL)	4×10^5	$2–5 \times 10^7$
	time (h)	16–24	1
HSPCs	concentration (cells/mL)	10^6	10^8
	time (h)	2–4	1

Associated with Figure 4A.

relevant AAV serotypes, including AAV6, have been found in a variety of animal models, including nonhuman primates, rodents, dogs, sheep, cats, horses, and pigs.[45–52] While dose-dependent inhibition of AAV transduction by FBS has been previously reported,[45] we are not aware of any studies that have definitively described the presence of anti-AAV NABs in FBS.

We also investigated the impact of other culture conditions on AAV6 transduction. In line with previous reports,[38] we found that increasing cell density by reducing the volume of media could greatly enhance AAV6 transduction. We were able to culture 10^6 primary hematopoietic cells in volumes as small as 10 μL using 96-well U-bottom plates (10^8 cells/mL, ~100-fold greater than a standard culture concentration), with minimal impact on cell viability during a 1 h transduction. Our results suggest that initial cell viability was not impaired by the optimized protocol in any of the cell types tested, though there may be longer-term impacts on cellular proliferative capacity that were not analyzed here. Some studies have described low-density culture methods (10^5 cells/mL) for HSPCs that enhance HDR, likely due to increased cellular proliferation.[10,21,53] However, as those studies also involved temporary higher cell densities (10^6 cells/mL) for AAV6 transduction,[21] we do not believe that our short 1 h AAV6 transduction at high cell density would preclude these sorts of optimizations, though further studies would be required to demonstrate this.

The observed impact of a short incubation period in lymphocytes matched our observations in K562 cells. Here, most of the benefits of AAV6 transduction at high densities were realized during the first hour, in an initial logarithmic phase that then tapered off to further increase transduction at only a linear rate. This biphasic pattern of AAV6 transduction could represent an initial excess of molecules involved in AAV6 attachment or entry, allowing a rapid initial burst of transduction, followed by a slower, linear phase that could be dependent on recycling or *de novo* synthesis of these receptors. In agreement with this model, previous studies using AAV2 and adherent cells have suggested that endocytosis may be a rate-limiting step in AAV transduction.[54,55] However, the reported kinetics of AAV uptake have varied,[37,54,56,57] perhaps reflecting differences in detection methods (physical labeling of particles versus productive gene expression), AAV serotype, or the endocytic pathway used. Several different endocytic pathways have all been implicated in AAV uptake, and usage may vary across cell types.[58,59] The unique biphasic transduction kinetics revealed here by an extended AAV6 transduction timeline in K562 cells warrants further study to confirm these findings and elucidate the mechanisms involved, which could lead to novel methods to modulate the rate of AAV endocytosis in cells.

The importance of endocytosis in this system is also reflected in the ability of electroporation to increase AAV transduction independent of the presence of a targeted nuclease. Charlesworth et al.[21] have previously suggested that electroporation prior to AAV6 transduction can prime cells to increase endocytosis, allowing greater AAV6 uptake through AAVR-mediated pathways. Similarly, we observed that electroporation enhanced AAV6 transduction of K562 cells, with the additional finding that this enhancement occurred regardless of whether AAV6 was added to cells before or after electroporation. Moreover, when cells were exposed to AAV6 prior to electroporation, transduction was dependent on viral attachment. The lack of effect of washing unbound AAV6 out prior to electroporation suggests enhanced entry of viral particles already attached to the cell rather than, for example, a bulk effect on direct membrane permeation caused by electroporation.

Based on the findings in K562 cells, we designed an optimized protocol for AAV6 transduction of hematopoietic cells that comprised a 1 h incubation in concentrated cell culture conditions in serum-free media, followed by electroporation with ZFN mRNA, and then a switch to culture in serum-containing media immediately afterward. We believe this timing maximizes AAV6 transduction while minimizing the potential negative impacts of serum starvation or cell overcrowding. Since our results here suggest that electroporation can enhance AAV transduction even after cells are exposed to the vector, and we have previously shown that this sequence of events is compatible with site-specific genome editing,[2] we chose to transduce the cells prior to electroporation. In this way, the high-density culture is performed when the cells are fully healthy rather than recovering from the harsher electroporation procedure.

We compared this optimized protocol to typical protocols described in the literature,[13,14,16] with the addition that the AAV6 transduction step was always performed in the absence of FBS. In both primary human T and B cells, we observed significant advantages with the optimized protocol compared to a protocol involving overnight serum-free AAV transduction following electroporation, both in cell viability and genome editing efficiency. Specifically, editing rates were improved by up to 7-fold in T cells and 21-fold in B cells at comparable MOIs, and similar editing frequencies were achieved with 50- to 100-fold less AAV6 per cell. These improvements could therefore significantly reduce the amount of AAV6 that would be required for *ex vivo* genome editing of lymphocytes, which could provide significant cost savings. This was especially apparent in B cells, where the

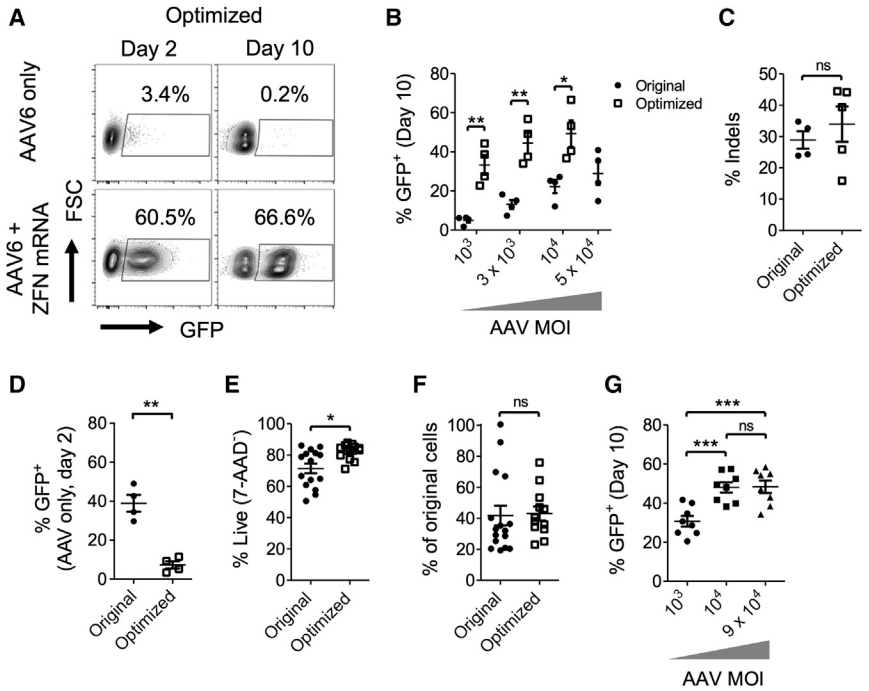

Figure 5. Improved genome editing in CD4⁺ T cells with an optimized protocol

(A–F) CD4⁺ T cells from n = 4 human donors were genome edited with either a previously published (original) or optimized protocol at the indicated AAV6-CCR5-GFP MOIs. (A) Representative plots of GFP expression measured by flow cytometry at days 2 and 10 for cells treated with the optimized protocol, with or without ZFN mRNA electroporation. (B) Stable genome editing shown by GFP expression at day 10. (C) Indel formation at *CCR5* by cells electroporated with ZFN mRNA with either protocol. (D) AAV6 transduction with either protocol was measured by flow cytometry for GFP at day 2 in samples treated with AAV6 but not ZFN mRNA at the highest MOI for each protocol (original = 5×10^4, optimized = 10^4). (E and F) Cell viability (E) and total cell counts by hemocytometer (F, normalized to the original number of cells prior to genome editing) were measured 1 day after genome editing. Conditions were pooled across AAV6 MOIs. (G) CD4⁺ T cells from n = 8 human donors were genome edited with the optimized protocol at indicated MOIs, and stable genome editing was measured by GFP expression at day 10. Data are shown as mean ± SEM. *p < 0.05; **p < 0.01; ***p < 0.001; and ns, not significant.

difficulty in transducing these cells with AAV6 means that MOIs of 10^6 are required without our optimized high-density transduction protocol. At such an MOI, editing 1 million cells *ex vivo* would require 10^{12} vg of vector, which is 10–100 times more AAV than used for some therapeutic doses for *in vivo* hepatic gene transfer in mice.[60]

Our data also highlight the impact of factors beyond AAV6 transduction on the efficiency of HDR-mediated genome editing, since an upper limit of editing rates clearly existed that could not be surpassed by increasing the AAV6 MOI. Other factors involved include the rate of DSB induction by the targeted nuclease, the influence of local DNA sequence on the choice of DNA repair pathway used,[61] and the activity of HDR repair pathways as a function of the cell cycle.[25] This last point may be of particular relevance, as the overnight serum starvation in the original protocols may have caused significant growth arrest and exit from the cell cycle into a G_0 phase[41] that does not support HDR. This could limit the ability to convert AAV6 transduction into site-specific genome editing and may at least partially explain the advantage of the optimized protocol that does not involve prolonged serum deprivation. Superior serum-free media formulations may be better able to support cell growth while avoiding serum-mediated inhibition of AAV transduction.

Indeed, the use of more effective serum-free media in HSPCs is one hypothesis for why the optimized protocol was not able to enhance genome editing in these cells, in contrast to findings in CD4⁺ T cells and B cells. Although serum-containing media was used after genome editing in HSPCs for historical reasons and to maintain similarities between the cell types studied in this manuscript, we (not shown) and others[11] have found that the serum-free media used here can efficiently support growth of HSPCs without additional FBS supplementation. Thus, cells may have been healthier after the original protocol and better able to undergo HDR-mediated genome editing, reducing a potential advantage of the optimized protocol. Alternatively, the lack of improvement with the optimized protocol in HSPCs may reflect the much greater permissivity of these cells to AAV6 transduction. Compared with MOIs of 5×10^4 in T cells and 10^6 in B cells, only 3×10^3 vg/cell were originally required for efficient genome editing in HSPCs. Our findings in K562 cells suggest that the impact of reduced media volumes is less dramatic at lower AAV MOIs across the conditions tested, perhaps suggesting that significantly lower volumes would be required to see an improvement in AAV transduction at lower MOIs in HSPCs.

In summary, we empirically tested cell culture parameters for their impact on transduction of hematopoietic cells by AAV6 vectors and used these findings to design an optimized protocol for genome editing. In primary human T and B lymphocytes, this approach significantly improved site-specific genome editing in conjunction with electroporation of ZFN mRNA, and we have also observed similar effects when using electroporation of CRISPR-Cas9 RNPs (data not shown). The dramatic differences we observed across protocols suggest that more detailed reports of cell culture and AAV transduction methodology may be necessary to ensure good reproducibility across labs. Our results also highlight the importance of cell-intrinsic factors and optimizing growth conditions to enable the highest rates of *ex vivo* genome editing and suggest that improved serum-free media may be required for continuing enhancements in

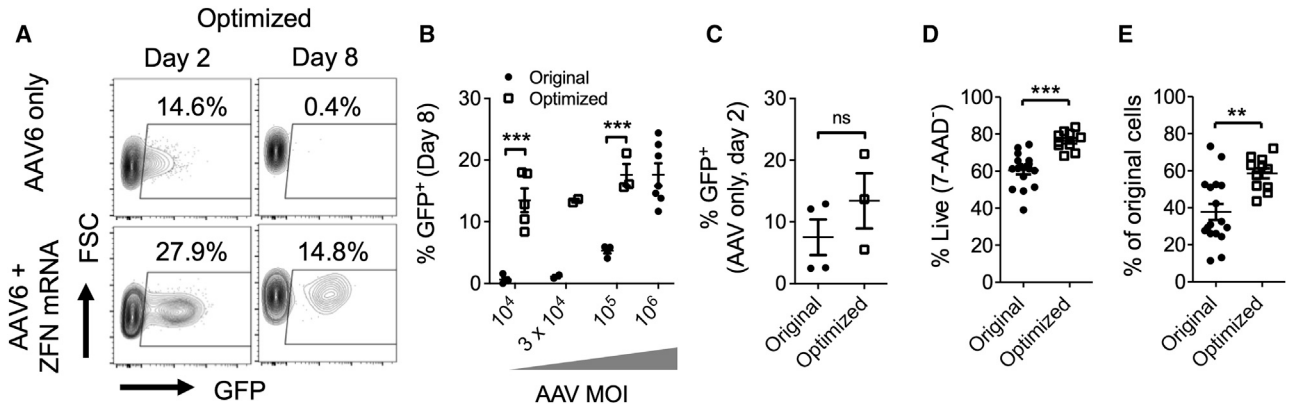

Figure 6. Improved genome editing in B cells with an optimized protocol

CD19+ B cells from n = 2–6 human donors were edited with either the original or optimized protocols at the indicated AAV6-CCR5-GFP MOIs. (A) Representative plots of GFP expression measured by flow cytometry at days 2 and 8 for cells treated with the optimized protocol, with or without ZFN mRNA electroporation. (B) Stable genome editing shown by GFP expression at day 8. (C) AAV6 transduction with either protocol was measured by flow cytometry for GFP at day 2 in samples treated with AAV6 but not ZFN mRNA at the highest MOI for each protocol (original = 10^6, optimized = 10^5). (D and E) Cell viability (D) and total cell counts by hemocytometer (E, normalized to the original number of cells prior to genome editing) were measured 1 day after genome editing. Conditions were pooled across AAV6 MOIs. Data are shown as mean ± SEM. **p < 0.01; ***p < 0.001.

ex vivo genome editing. Nevertheless, these procedures may be a useful starting point for investigators using AAV6 for site-specific genome editing in hematopoietic cells.

MATERIALS AND METHODS

AAV vectors

AAV6-CCR5-GFP vectors containing AAV2 ITRs, *CCR5* homology arms of 473 bp (left) and 1,431 bp (right), a hPGK promoter driving eGFP, and a BGH polyA signal were produced as previously described[2] and generously provided by Sangamo Therapeutics. AAV1-CMV-GFP and AAV2-CMV-GFP vectors were purchased from Vigene Biosciences (Rockville, MD, USA). AAV vectors were titrated as previously described,[36] and protocols are provided in the supplemental methods.

Cell line culture, AAV transduction, and electroporation

HEK293T cells and HeLa cells were cultured in DMEM supplemented with 10% FBS and 1% penicillin/streptomycin. Cells were seeded overnight to adhere to plates and washed once with PBS prior to AAV transduction in DMEM, with or without FBS or human AB serum. FBS was heat-inactivated at 56°C water bath for 30 min. AAV vectors were added to cells at indicated MOIs, and after 4 h at 37°C, 10% FBS (final volume) was restored to the culture if appropriate.

K562, Raji, and Molt4.8 cells were cultured in RPMI-1640 medium supplemented with 10% FBS and 1% penicillin/streptomycin. Cells were washed twice with PBS, seeded into plates at indicated cell concentrations in RPMI-1640, with or without FBS or human AB serum, and transduced with AAV vectors at indicated MOIs at 37°C. After 2 h (or as indicated), 10% FBS (final volume) was restored to the culture if appropriate. Electroporation of K562 cells was performed using a SF Cell Line 4D-Nucleofector kit and 4D-X Nucleofector using pulse code FF-120 (Lonza, Basel, Switzerland), per the manufacturer's recommendations. After 2 days, GFP expression was measured by flow cytometry, and vector copy numbers were measured by Droplet Digital PCR (ddPCR) as previously described.[36] Detailed protocols for AAV copy number determination are provided in the supplemental methods.

Viral attachment assay

K562 cells were washed with PBS, resuspended in RPMI-1640 with or without 10% FBS, and incubated at 4°C for 30 min at 10^6 cells/mL. AAV6-CCR5-GFP vectors were added at an MOI of 10^4 and allowed to attach to the cells for 1 h at 4°C. Cells were washed at 4°C to remove unattached AAV6 virions, resuspended in RPMI-1640 with or without 10% FBS as indicated, and incubated at 37°C. Control samples were also transduced with AAV6-CCR5-GFP in FBS-free RPMI-1640 at the same MOI and cell concentration. After allowing transduction for 2 h, samples without FBS were supplemented with 10% FBS, and cells were cultured for 2 days at 37°C.

Human CD4+ T cells

Human buffy coat preparations were obtained from Gulf Coast Regional Blood Center (Houston, TX, USA). PBMCs were isolated by Ficoll-Paque (GE Healthcare Life Sciences, Marlborough, MA, USA) density centrifugation using Leucosep tubes (Greiner Bio-One, Kremsmünster, Austria), and platelets were reduced by low-speed washing. Human CD4+ T cells were isolated by positive magnetic selection using human CD4 MicroBeads kit (Miltenyi Biotec, Bergisch Gladbach, Germany) per manufacturer's instructions. For activation, purified CD4+ T cells were cultured at 2 × 10^6 cells/mL in T cell media: X-VIVO-15 media supplemented

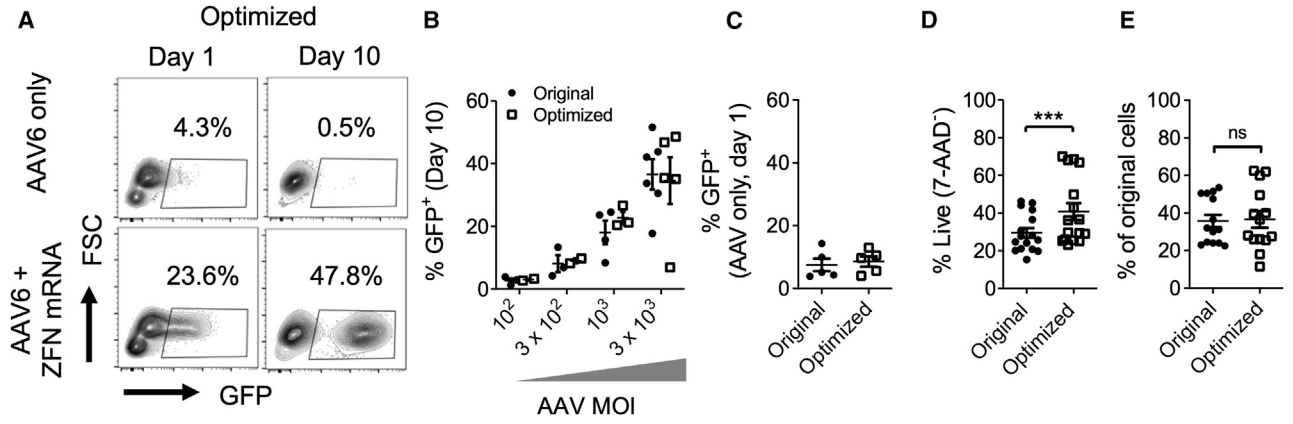

Figure 7. Comparable efficacy of both protocols in HSPCs

CD34+ HSPCs from n = 2–6 human donors were edited with either an original or optimized protocol at the indicated AAV6-CCR5-GFP MOIs. (A) Representative plots of GFP expression measured by flow cytometry at days 1 and 10 for cells treated with the optimized protocol, with or without ZFN mRNA electroporation. (B) Stable genome editing rates, shown by GFP expression at day 10. (C) AAV6 transduction with either protocol was measured by flow cytometry for GFP at day 1 in samples treated with AAV6 but not ZFN mRNA at the highest AAV MOI (3×10^3). (D and E) Cell viability (D) and total cell counts by hemocytometer (E, normalized to the original number of cells prior to genome editing) were measured 1 day after genome editing. Conditions were pooled across AAV6 MOIs. Data are shown as mean ± SEM. ***$p < 0.001$.

with 10% FBS, 2 mM L-glutamine, 1% penicillin/streptomycin/amphotericin B (Sigma-Aldrich), 20 ng/mL IL-2 (Peprotech, Rocky Hill, NJ, USA), and Dynabeads Human T-Activator CD3/CD28 (Thermo Fisher) at 1 bead per cell, as previously described.[13] After 3 days, beads were removed using a DynaMag-2 (Thermo Fisher) per manufacturer's instructions. Cells were washed twice with PBS and then genome edited with indicated protocols.

Human B cells

Frozen human peripheral blood CD19+ B cells were purchased from StemCell Technologies (Vancouver, BC, Canada). Cells were thawed per manufacturer's instructions and cultured as previously described.[62] Briefly, cells were initially activated at 4×10^5–10^6 cells/mL in B cell activation media: Iscove's modified Dulbecco's medium (IMDM, Corning, Corning, NY, USA) supplemented with 10% FBS, 5 μg/mL soluble CD40L (R&D Systems, Minneapolis, MN, USA), 10 μg/mL anti-His tag antibody (clone AD1.1.10, R&D Systems), 50 ng/mL CpG ODN 2006 (Invivogen, San Diego, CA, USA), 10 ng/mL IL-2 (R&D Systems), 50 ng/mL IL-10, and 10 ng/mL IL-15 (Peprotech). After 2 days of activation, cells were washed twice with PBS and then genome edited with indicated protocols.

After genome editing, cells were cultured an additional 2 days in B cell activation media. Then, cells were pelleted by centrifugation, and media was replaced with plasmablast generation media: IMDM supplemented with 10% FBS, 10 ng/mL IL-2 (R&D Systems), 50 ng/mL IL-6 (Peprotech), 50 ng/mL IL-10, and 10 ng/mL IL-15. After a further 3 days of culture, cells were pelleted by centrifugation and media was replaced with plasma cell generation media: IMDM supplemented with 10% FBS, 50 ng/mL IL-6, 10 ng/mL IL-15, and 500 U/mL IFN-α (R&D Systems). Cells were cultured in this media for 3 additional days.

Human CD34+ HSPCs

Fetal liver CD34+ HSPCs were isolated from tissue obtained from Advanced Bioscience Resources (Alameda, CA, USA) as anonymous waste samples, with approval of the University of Southern California's Institutional Review Board. CD34+ cells were isolated as previously described,[2] using physical disruption, incubation in collagenase to give single-cell suspensions, and magnetic bead selection using an EasySep Human CD34 Positive Selection Kit (STEMCELL Technologies). The resulting CD34+ HSPCs were cultured in HSPC media: StemSpan SFEM II (STEMCELL Technologies) supplemented with 1% penicillin/streptomycin/amphotericin B and SFT cytokines: 50 ng/mL each of SCF, Flt3 ligand and TPO (R&D Systems). After overnight pre-stimulation, HSPCs were washed twice with PBS and then genome edited with indicated protocols.

Genome editing protocols

Protocols for preparation of ZFN reagents, measurement of indels, and detailed protocols for genome editing of K562 cells, human CD4 T cells, human B cells, and human HSPCs are provided in the supplemental methods.

Flow cytometry

GFP expression was measured by flow cytometry as indicated on either a FACSCanto II (BD Biosciences, San Diego, CA, USA) or Guava easyCyte (MilliporeSigma, Burlington, MA, USA). Viability was measured by 7-AAD staining (BD Biosciences). Data were analyzed using FlowJo software (Flowjo, Ashland, OR, USA).

Statistics

Results are reported as mean ± standard error of the mean (SEM). Significant differences between groups were determined with unpaired Student's t test, one-way analysis of variance with Tukey post-tests, two-way analysis of variance with Bonferroni post-tests,

linear regression, or semilogarithmic regression, as appropriate. p values < 0.05 were considered significant. Analyses were performed using GraphPad Prism software (San Diego, CA, USA). Differences are indicated as * $p < 0.05$; ** $p < 0.01$; *** $p < 0.001$; and ns, not significant.

SUPPLEMENTAL INFORMATION

Supplemental information can be found online at https://doi.org/10.1016/j.omtm.2021.09.003.

ACKNOWLEDGMENTS

We would like to thank B. Riley, M. Holmes, and Sangamo Therapeutics Inc. for providing AAV6-CCR5-GFP vectors, *CCR5* ZFN reagents, and discussions about methods for B cell culture and genome editing. This work was supported by National Institutes of Health grants HL129902 and HL156274 to P.M.C. G.L.R. was supported by a Career Development Award from the American Society of Gene & Cell Therapy. The content is solely the responsibility of the authors and does not necessarily represent the official views of the American Society of Gene & Cell Therapy. H.-Y.C. was supported by a Taiwan USC scholarship.

AUTHOR CONTRIBUTIONS

G.L.R., C.H., and R.D.E.C. performed experiments. G.L.R. and P.M.C. designed experiments and analyzed and interpreted data. E.S. and H.-Y.C. contributed to discussions. G.L.R. and P.M.C. wrote the manuscript. P.M.C. supervised the study.

DECLARATION OF INTERESTS

The authors declare no competing interests.

REFERENCES

1. Hirakawa, M.P., Krishnakumar, R., Timlin, J.A., Carney, J.P., and Butler, K.S. (2020). Gene editing and CRISPR in the clinic: current and future perspectives. Biosci. Rep. *40*, BSR20200127.
2. Wang, J., Exline, C.M., DeClercq, J.J., Llewellyn, G.N., Hayward, S.B., Li, P.W., Shivak, D.A., Surosky, R.T., Gregory, P.D., Holmes, M.C., and Cannon, P.M. (2015). Homology-driven genome editing in hematopoietic stem and progenitor cells using ZFN mRNA and AAV6 donors. Nat. Biotechnol. *33*, 1256–1263.
3. Sather, B.D., Romano Ibarra, G.S., Sommer, K., Curinga, G., Hale, M., Khan, I.F., Singh, S., Song, Y., Gwiazda, K., Sahni, J., et al. (2015). Efficient modification of CCR5 in primary human hematopoietic cells using a megaTAL nuclease and AAV donor template. Sci. Transl. Med. *7*, 307ra156.
4. Dever, D.P., Bak, R.O., Reinisch, A., Camarena, J., Washington, G., Nicolas, C.E., Pavel-Dinu, M., Saxena, N., Wilkens, A.B., Mantri, S., et al. (2016). CRISPR/Cas9 β-globin gene targeting in human haematopoietic stem cells. Nature *539*, 384–389.
5. Bak, R.O., Gomez-Ospina, N., and Porteus, M.H. (2018). Gene Editing on Center Stage. Trends Genet. *34*, 600–611.
6. Jasin, M., and Rothstein, R. (2013). Repair of strand breaks by homologous recombination. Cold Spring Harb. Perspect. Biol. *5*, a012740.
7. Kan, Y., Ruis, B., Lin, S., and Hendrickson, E.A. (2014). The mechanism of gene targeting in human somatic cells. PLoS Genet. *10*, e1004251.
8. Romero, Z., Lomova, A., Said, S., Miggelbrink, A., Kuo, C.Y., Campo-Fernandez, B., Hoban, M.D., Masiuk, K.E., Clark, D.N., Long, J., et al. (2019). Editing the Sickle Cell Disease Mutation in Human Hematopoietic Stem Cells: Comparison of Endonucleases and Homologous Donor Templates. Mol. Ther. *27*, 1389–1406.
9. Park, S.H., Lee, C.M., Dever, D.P., Davis, T.H., Camarena, J., Srifa, W., Zhang, Y., Paikari, A., Chang, A.K., Porteus, M.H., et al. (2019). Highly efficient editing of the β-globin gene in patient-derived hematopoietic stem and progenitor cells to treat sickle cell disease. Nucleic Acids Res. *47*, 7955–7972.
10. Pavel-Dinu, M., Wiebking, V., Dejene, B.T., Srifa, W., Mantri, S., Nicolas, C.E., Lee, C., Bao, G., Kildebeck, E.J., Punjya, N., et al. (2019). Gene correction for SCID-X1 in long-term hematopoietic stem cells. Nat. Commun. *10*, 1634.
11. Schiroli, G., Conti, A., Ferrari, S., Della Volpe, L., Jacob, A., Albano, L., Beretta, S., Calabria, A., Vavassori, V., Gasparini, P., et al. (2019). Precise Gene Editing Preserves Hematopoietic Stem Cell Function following Transient p53-Mediated DNA Damage Response. Cell Stem Cell *24*, 551–565.e8.
12. Ferrari, S., Jacob, A., Beretta, S., Unali, G., Albano, L., Vavassori, V., Cittaro, D., Lazarevic, D., Brombin, C., Cugnata, F., et al. (2020). Efficient gene editing of human long-term hematopoietic stem cells validated by clonal tracking. Nat. Biotechnol. *38*, 1298–1308.
13. Wang, J., DeClercq, J.J., Hayward, S.B., Li, P.W., Shivak, D.A., Gregory, P.D., Lee, G., and Holmes, M.C. (2016). Highly efficient homology-driven genome editing in human T cells by combining zinc-finger nuclease mRNA and AAV6 donor delivery. Nucleic Acids Res. *44*, e30.
14. Eyquem, J., Mansilla-Soto, J., Giavridis, T., van der Stegen, S.J., Hamieh, M., Cunanan, K.M., Odak, A., Gönen, M., and Sadelain, M. (2017). Targeting a CAR to the TRAC locus with CRISPR/Cas9 enhances tumour rejection. Nature *543*, 113–117.
15. Wiebking, V., Lee, C.M., Mostrel, N., Lahiri, P., Bak, R., Bao, G., Roncarolo, M.G., Bertaina, A., and Porteus, M.H. (2021). Genome editing of donor-derived T-cells to generate allogenic chimeric antigen receptor-modified T cells: Optimizing alpha-beta T cell-depleted haploidentical hematopoietic stem cell transplantation. Haematologica *106*, 847–858.
16. Hung, K.L., Meitlis, I., Hale, M., Chen, C.Y., Singh, S., Jackson, S.W., Miao, C.H., Khan, I.F., Rawlings, D.J., and James, R.G. (2018). Engineering Protein-Secreting Plasma Cells by Homology-Directed Repair in Primary Human B Cells. Mol. Ther. *26*, 456–467.
17. Moffett, H.F., Harms, C.K., Fitzpatrick, K.S., Tooley, M.R., Boonyaratanakornkit, J., and Taylor, J.J. (2019). B cells engineered to express pathogen-specific antibodies protect against infection. Sci. Immunol. *4*, eaax0644.
18. Hartweger, H., McGuire, A.T., Horning, M., Taylor, J.J., Dosenovic, P., Yost, D., Gazumyan, A., Seaman, M.S., Stamatatos, L., Jankovic, M., and Nussenzweig, M.C. (2019). HIV-specific humoral immune responses by CRISPR/Cas9-edited B cells. J. Exp. Med. *216*, 1301–1310.
19. Nahmad, A.D., Raviv, Y., Horovitz-Fried, M., Sofer, I., Akriv, T., Nataf, D., Dotan, I., Carmi, Y., Burstein, D., Wine, Y., et al. (2020). Engineered B cells expressing an anti-HIV antibody enable memory retention, isotype switching and clonal expansion. Nat. Commun. *11*, 5851.
20. Huang, D., Tran, J.T., Olson, A., Vollbrecht, T., Tenuta, M., Guryleva, M.V., Fuller, R.P., Schiffner, T., Abadejos, J.R., Couvrette, L., et al. (2020). Vaccine elicitation of HIV broadly neutralizing antibodies from engineered B cells. Nat. Commun. *11*, 5850.
21. Charlesworth, C.T., Camarena, J., Cromer, M.K., Vaidyanathan, S., Bak, R.O., Carte, J.M., Potter, J., Dever, D.P., and Porteus, M.H. (2018). Priming Human Repopulating Hematopoietic Stem and Progenitor Cells for Cas9/sgRNA Gene Targeting. Mol. Ther. Nucleic Acids *12*, 89–104.
22. Lattanzi, A., Meneghini, V., Pavani, G., Amor, F., Ramadier, S., Felix, T., Antoniani, C., Masson, C., Alibeu, O., Lee, C., et al. (2019). Optimization of CRISPR/Cas9 Delivery to Human Hematopoietic Stem and Progenitor Cells for Therapeutic Genomic Rearrangements. Mol. Ther. *27*, 137–150.
23. Broeders, M., Herrero-Hernandez, P., Ernst, M.P.T., van der Ploeg, A.T., and Pijnappel, W.W.M.P. (2020). Sharpening the Molecular Scissors: Advances in Gene-Editing Technology. iScience *23*, 100789.
24. Hendel, A., Bak, R.O., Clark, J.T., Kennedy, A.B., Ryan, D.E., Roy, S., Steinfeld, I., Lunstad, B.D., Kaiser, R.J., Wilkens, A.B., et al. (2015). Chemically modified guide RNAs enhance CRISPR-Cas genome editing in human primary cells. Nat. Biotechnol. *33*, 985–989.

25. Lomova, A., Clark, D.N., Campo-Fernandez, B., Flores-Bjurström, C., Kaufman, M.L., Fitz-Gibbon, S., Wang, X., Miyahira, E.Y., Brown, D., DeWitt, M.A., et al. (2019). Improving Gene Editing Outcomes in Human Hematopoietic Stem and Progenitor Cells by Temporal Control of DNA Repair. Stem Cells *37*, 284–294.

26. De Ravin, S.S., Brault, J., Meis, R.J., Liu, S., Li, L., Pavel-Dinu, M., Lazzarotto, C.R., Liu, T., Koontz, S.M., Choi, U., et al. (2021). Enhanced homology-directed repair for highly efficient gene editing in hematopoietic stem/progenitor cells. Blood *137*, 2598–2608.

27. Pattabhi, S., Lotti, S.N., Berger, M.P., Singh, S., Lux, C.T., Jacoby, K., Lee, C., Negre, O., Scharenberg, A.M., and Rawlings, D.J. (2019). In Vivo Outcome of Homology-Directed Repair at the HBB Gene in HSC Using Alternative Donor Template Delivery Methods. Mol. Ther. Nucleic Acids *17*, 277–288.

28. Halder, S., Ng, R., and Agbandje-McKenna, M. (2012). Parvoviruses: structure and infection. Future Virol. *7*, 253–278.

29. Kumar, S.R., Markusic, D.M., Biswas, M., High, K.A., and Herzog, R.W. (2016). Clinical development of gene therapy: results and lessons from recent successes. Mol. Ther. Methods Clin. Dev. *3*, 16034.

30. Dunbar, C.E., High, K.A., Joung, J.K., Kohn, D.B., Ozawa, K., and Sadelain, M. (2018). Gene therapy comes of age. Science *359*, eaan4672.

31. Mingozzi, F., and High, K.A. (2011). Therapeutic in vivo gene transfer for genetic disease using AAV: progress and challenges. Nat. Rev. Genet. *12*, 341–355.

32. Song, L., Kauss, M.A., Kopin, E., Chandra, M., Ul-Hasan, T., Miller, E., Jayandharan, G.R., Rivers, A.E., Aslanidi, G.V., Ling, C., et al. (2013). Optimizing the transduction efficiency of capsid-modified AAV6 serotype vectors in primary human hematopoietic stem cells in vitro and in a xenograft mouse model in vivo. Cytotherapy *15*, 986–998.

33. Song, L., Li, X., Jayandharan, G.R., Wang, Y., Aslanidi, G.V., Ling, C., Zhong, L., Gao, G., Yoder, M.C., Ling, C., et al. (2013). High-efficiency transduction of primary human hematopoietic stem cells and erythroid lineage-restricted expression by optimized AAV6 serotype vectors in vitro and in a murine xenograft model in vivo. PLoS ONE *8*, e58757.

34. Yang, H., Qing, K., Keeler, G.D., Yin, L., Mietzsch, M., Ling, C., Hoffman, B.E., Agbandje-McKenna, M., Tan, M., Wang, W., and Srivastava, A. (2020). Enhanced Transduction of Human Hematopoietic Stem Cells by AAV6 Vectors: Implications in Gene Therapy and Genome Editing. Mol. Ther. Nucleic Acids *20*, 451–458.

35. Wang, M., Sun, J., Crosby, A., Woodard, K., Hirsch, M.L., Samulski, R.J., and Li, C. (2017). Direct interaction of human serum proteins with AAV virions to enhance AAV transduction: immediate impact on clinical applications. Gene Ther. *24*, 49–59.

36. Rogers, G.L., Chen, H.Y., Morales, H., and Cannon, P.M. (2019). Homologous Recombination-Based Genome Editing by Clade F AAVs Is Inefficient in the Absence of a Targeted DNA Break. Mol. Ther. *27*, 1726–1736.

37. Bartlett, J.S., Wilcher, R., and Samulski, R.J. (2000). Infectious entry pathway of adeno-associated virus and adeno-associated virus vectors. J. Virol. *74*, 2777–2785.

38. Ling, C., Bhukhai, K., Yin, Z., Tan, M., Yoder, M.C., Leboulch, P., Payen, E., and Srivastava, A. (2016). High-Efficiency Transduction of Primary Human Hematopoietic Stem/Progenitor Cells by AAV6 Vectors: Strategies for Overcoming Donor-Variation and Implications in Genome Editing. Sci. Rep. *6*, 35495.

39. Schlesinger, M. (1932). Adsorption of phages to homologous bacteria. II. Quantitative investigations of adsorption velocity and saturation. Estimation of the particle size of the bacteriophage. In Papers on Bacterial Viruses,, G.S. Stent, ed. (Boston, Mass.: Little Brown and Company), pp. 26–36.

40. Lang, J.F., Toulmin, S.A., Brida, K.L., Eisenlohr, L.C., and Davidson, B.L. (2019). Standard screening methods underreport AAV-mediated transduction and gene editing. Nat. Commun. *10*, 3415.

41. Pardee, A.B. (1989). G1 events and regulation of cell proliferation. Science *246*, 603–608.

42. Rogers, G.L., Martino, A.T., Aslanidi, G.V., Jayandharan, G.R., Srivastava, A., and Herzog, R.W. (2011). Innate Immune Responses to AAV Vectors. Front. Microbiol. *2*, 194.

43. Piras, F., and Kajaste-Rudnitski, A. (2021). Antiviral immunity and nucleic acid sensing in haematopoietic stem cell gene engineering. Gene Ther. *28*, 16–28.

44. Russell, D.W., Miller, A.D., and Alexander, I.E. (1994). Adeno-associated virus vectors preferentially transduce cells in S phase. Proc. Natl. Acad. Sci. USA *91*, 8915–8919.

45. Rapti, K., Louis-Jeune, V., Kohlbrenner, E., Ishikawa, K., Ladage, D., Zolotukhin, S., Hajjar, R.J., and Weber, T. (2012). Neutralizing antibodies against AAV serotypes 1, 2, 6, and 9 in sera of commonly used animal models. Mol. Ther. *20*, 73–83.

46. Shin, J.H., Yue, Y., Smith, B., and Duan, D. (2012). Humoral immunity to AAV-6, 8, and 9 in normal and dystrophic dogs. Hum. Gene Ther. *23*, 287–294.

47. Tellez, J., Van Vliet, K., Tseng, Y.S., Finn, J.D., Tschernia, N., Almeida-Porada, G., Arruda, V.R., Agbandje-McKenna, M., and Porada, C.D. (2013). Characterization of naturally-occurring humoral immunity to AAV in sheep. PLoS ONE *8*, e75142.

48. Calcedo, R., Franco, J., Qin, Q., Richardson, D.W., Mason, J.B., Boyd, S., and Wilson, J.M. (2015). Preexisting Neutralizing Antibodies to Adeno-Associated Virus Capsids in Large Animals Other Than Monkeys May Confound In Vivo Gene Therapy Studies. Hum. Gene Ther. Methods *26*, 103–105.

49. Calcedo, R., and Wilson, J.M. (2016). AAV Natural Infection Induces Broad Cross-Neutralizing Antibody Responses to Multiple AAV Serotypes in Chimpanzees. Hum. Gene Ther. Clin. Dev. *27*, 79–82.

50. Wang, D., Zhong, L., Li, M., Li, J., Tran, K., Ren, L., He, R., Xie, J., Moser, R.P., Fraser, C., et al. (2018). Adeno-Associated Virus Neutralizing Antibodies in Large Animals and Their Impact on Brain Intraparenchymal Gene Transfer. Mol. Ther. Methods Clin. Dev. *11*, 65–72.

51. Li, P., Boenzli, E., Hofmann-Lehmann, R., and Helfer-Hungerbuehler, A.K. (2019). Pre-existing antibodies to candidate gene therapy vectors (adeno-associated vector serotypes) in domestic cats. PLoS ONE *14*, e0212811.

52. Elmore, Z.C., Oh, D.K., Simon, K.E., Fanous, M.M., and Asokan, A. (2020). Rescuing AAV gene transfer from neutralizing antibodies with an IgG-degrading enzyme. JCI Insight *5*, e139881.

53. Bak, R.O., Dever, D.P., and Porteus, M.H. (2018). CRISPR/Cas9 genome editing in human hematopoietic stem cells. Nat. Protoc. *13*, 358–376.

54. Duan, D., Li, Q., Kao, A.W., Yue, Y., Pessin, J.E., and Engelhardt, J.F. (1999). Dynamin is required for recombinant adeno-associated virus type 2 infection. J. Virol. *73*, 10371–10376.

55. Sanlioglu, A.D., Karacay, B., Benson, P.K., Engelhardt, J.F., and Sanlioglu, S. (2004). Novel approaches to augment adeno-associated virus type-2 endocytosis and transduction. Virus Res. *104*, 51–59.

56. Murphy, S.L., Li, H., Zhou, S., Schlachterman, A., and High, K.A. (2008). Prolonged susceptibility to antibody-mediated neutralization for adeno-associated vectors targeted to the liver. Mol. Ther. *16*, 138–145.

57. Seisenberger, G., Ried, M.U., Endress, T., Büning, H., Hallek, M., and Bräuchle, C. (2001). Real-time single-molecule imaging of the infection pathway of an adeno-associated virus. Science *294*, 1929–1932.

58. Dhungel, B.P., Bailey, C.G., and Rasko, J.E.J. (2021). Journey to the Center of the Cell: Tracing the Path of AAV Transduction. Trends Mol. Med. *27*, 172–184.

59. Weinberg, M.S., Nicolson, S., Bhatt, A.P., McLendon, M., Li, C., and Samulski, R.J. (2014). Recombinant adeno-associated virus utilizes cell-specific infectious entry mechanisms. J. Virol. *88*, 12472–12484.

60. Cooper, M., Nayak, S., Hoffman, B.E., Terhorst, C., Cao, O., and Herzog, R.W. (2009). Improved induction of immune tolerance to factor IX by hepatic AAV-8 gene transfer. Hum. Gene Ther. *20*, 767–776.

61. Tatiossian, K.J., Clark, R.D.E., Huang, C., Thornton, M.E., Grubbs, B.H., and Cannon, P.M. (2021). Rational selection of CRISPR-Cas9 guide RNAs for homology-directed genome editing. Mol. Ther. *29*, 1057–1069..

62. Jourdan, M., Caraux, A., De Vos, J., Fiol, G., Larroque, M., Cognot, C., Bret, C., Duperray, C., Hose, D., and Klein, B. (2009). An in vitro model of differentiation of memory B cells into plasmablasts and plasma cells including detailed phenotypic and molecular characterization. Blood *114*, 5173–5181.